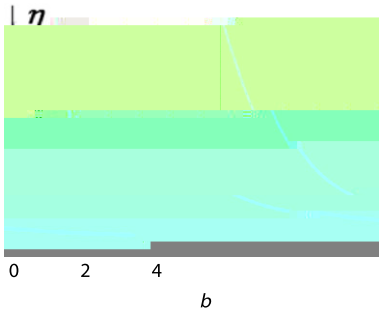

Fig. 3 – Relationship between parameters *b* and *η*.

3. Mass transport and mass exchange

Cell contractility relies on the mass exchange through the polymerization of G-actin monomers into actin laments that are a key597(n709 cuctu)18(acl-497(kcomponnts97(n70f)]497(kS)1829.)]7(n70These]497(k)12(e)ctinnsh-498(a))12(e)-TJ ET 1 0 0 1 52.441 531.628 Tm

procedures, such as micropipette aspiration, clearly exhibit a time-dependency that is usually attributed to a combination of the intrinsic visco-elasticity of the cytoskeleton and the ow driven deformation of the cytoplasm. In terms of cell morphology, it is likely that cytosol ow governs the number and size of cell protrusions. Indeed, Weiss and Garber (1952), in his analysis on the shape of mesemchymal cells, explained the development of cell extensions (or lopodia) in terms of competitive mechanisms based on the amount of cytosol each protrusion could intake. Complex interactions may exist between the transport and uid and that of dissolved species, which may result in a quite complex problem. However, it is important to make a few simplifying assumptions for the sake of clarity. The present analysis is then based on the following points. First, assuming that the concentration of G-actin in the cytosol is small, it is reasonable to say that actin monomer transport does not affect the interstitial ow of cytosol. In other words, cytosol ow can be expressed only in terms of a differential of pressure though Darcy's law as follows:

$$J^f = \frac{K}{\mu} \nabla p \tag{32}$$

where K

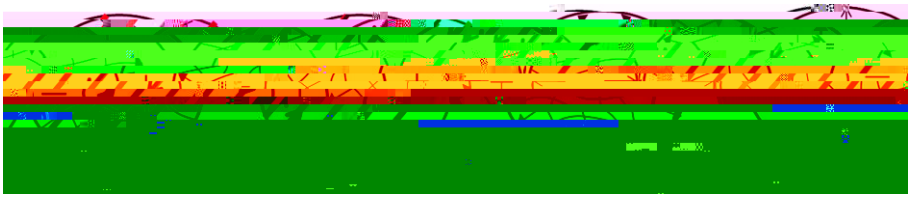

Fig. 4 – Decomposition of the Cauchy stress.

possess a sarcomeric structure similar to that found in myofibrils of muscle cells, contractile forces are very likely to be highly dependent on the strain-rate and current length of SF, as predicted by cross-bridge dynamics models (Carlson and Wilkie, 1974). To incorporate these mechanisms into the proposed model, this section concentrates on key mechanical aspects of the problem by (a) writing the force equilibrium between the four constituents present in the cell and (b) introducing constitutive relations for SF contraction and cytoskeleton deformation.

4.1. Mechanical equilibrium of the cell

Let us first consider the mechanical equilibrium of the cell by writing the balance of momentum associated with each constituent. Introducing T^{α} as the partial Cauchy stress associated with constituent α, the momentum balance forlo1 5s168 7.9(associat.327 (associated).327 (a01.327 2.44327 1 44te01.327 4(ynamics)-3

1690

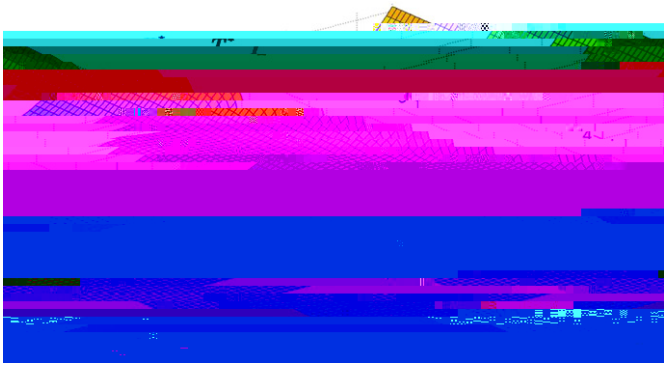

Fig. 7 – Three-dimensional representation of the cell contraction $T^{\star}$ as a function of SF strain ϵ/ϵ_0 and strain rate $\dot{\epsilon}^p/\dot{\epsilon}^0$.

We give a three-dimensional representation of contraction in terms of ϵ and $\dot{\epsilon}$ in Fig. 7.

Contraction of the SF network. The above model is able to characterize the contraction of a single SF but does not describe the contraction of an anisotropic network. This issue can be addressed by relating the contraction of a single SF to the contractile stress tensor $\mathbf{T}^p$, as follows. First, we write the uniaxial contractile stress T^p_θ in a specific direction θ in terms of the volume fraction of SF and the stress $T = \varphi T^?$ in each individual fiber as:

$$T^p_\theta = \varphi_\theta \varphi T^?. \tag{49}$$

Second, the stress tensor $\mathbf{T}^p$ is derived from the averaging equation defined in (38): $\mathbf{T}^p = \langle T^p_\theta \mathbf{m}_\theta \otimes \mathbf{m}_\theta \rangle$. Referring to the definition of the averaging operation (12), the stress $\mathbf{T}^p$ can then be found in terms of the Green–Lagrange strain tensor $\mathbf{E}$ and its material time derivative $\dot{\mathbf{E}}$ by computing the integral:

$$\mathbf{T}^p(\mathbf{E}, \dot{\mathbf{E}}) = \frac{\varphi}{\pi} \int_{\pi=2}^{\pi=2} \varphi^p_\theta T^?(\epsilon_\theta, \dot{\epsilon}_\theta) \mathbf{M}_\theta \, d\theta \tag{50}$$

where $\epsilon_\theta = \mathbf{E} : \mathbf{M}_\theta$ and $\dot{\epsilon}_\theta = \dot{\mathbf{E}} : \mathbf{M}_\theta$.

Here, we used the fact that the tensile strain (and its rate) in a certain direction can be found through a double tensor contraction ":" with the matrix $\mathbf{M}_\theta$. The above integral can be determined computationally using the Von Mises distribution and the state of strain and strain rate at a material point. Relation (50) therefore clearly establishes a link between contractile stress, fiber distribution and the underlying molecular mechanisms of the cross-bridge dynamics.

4.3. *Cytoskeleton elasticity*

According to the velocity–tension relation, it is clear that contractility is promoted by a scenario in which the rate of SF shortening is limited. There are two elements that contribute to the resistance of contractile deformation: the passive cytoskeleton and the underlying substrate (through cell-matrix attachments provided by focal adhesions). The passive cytoskeleton consists of a filamentous network that can resist actin contraction through the mechanical balance between compressive elements (microtubules), tensile elements (actin and intermediate

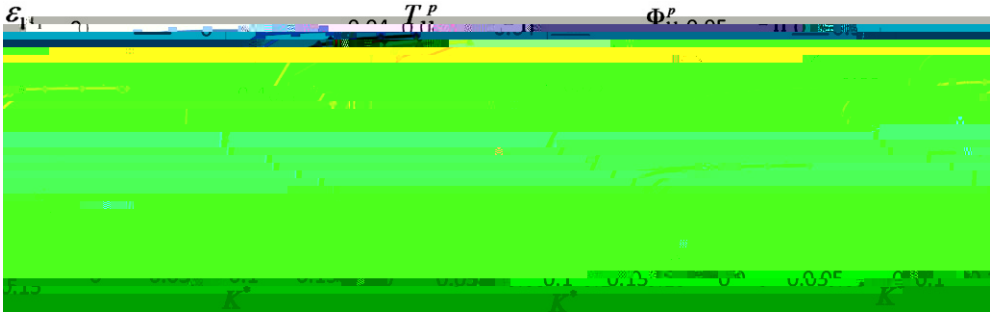

Fig. 11 – Effect of support stiffness on steady state cell deformation, contractile stress and SF anisotropy for different values of mechano-sensitivity coefficient $k1^{f*}$.

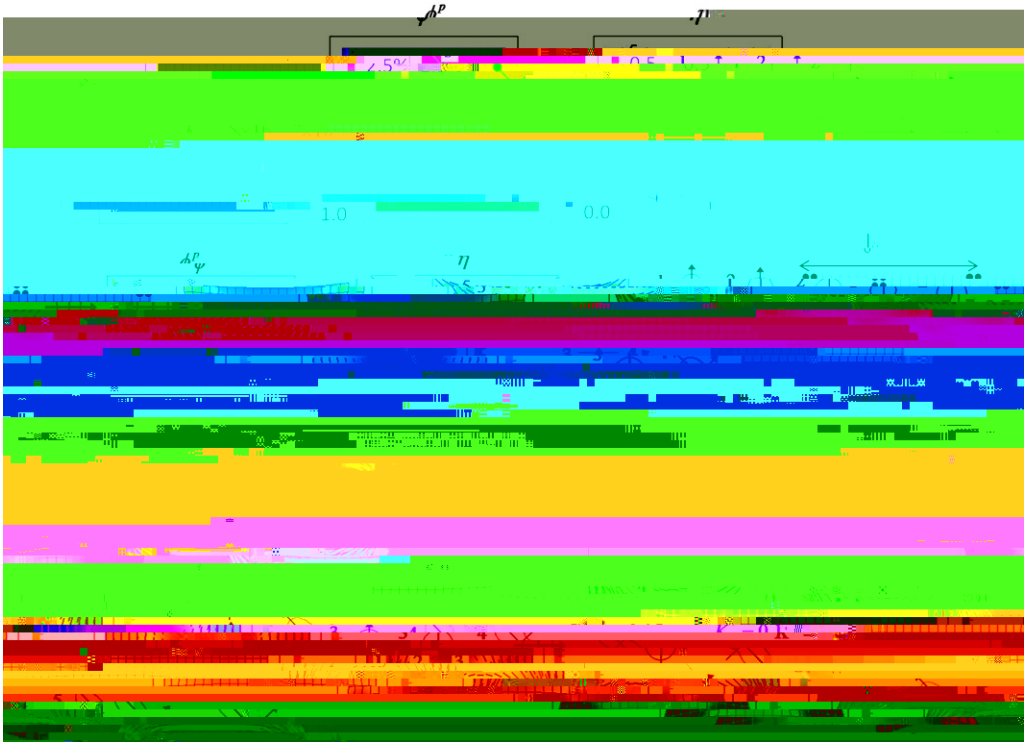

Fig. 12 – SF volume fraction φp and distribution at steady-state for three values of support stiffness (ranging from very low to very high). The principal direction of SFs are indicated by lines and the parameter η refers to the degree of anisotropy (η D 0.5 for an isotropic network and η D 0 for an unidirectional fiber direction). The polar fiber distribution (φ

Fig. 13 – Steady-state contractile force *F* at focal adhesions as a function of support stiffness *K* as predicted with the

Fig. 14 – Mechanical work of the cell in terms of substrate stiffness: Qualitative comparison of model prediction and experiments on cardiomyocytes (Adam et al., 2008).

show that the model captures both the order of magnitude of contractile forces as well as the trends in substrate stiffness-cell contraction relationships.

An important consequence of the observed behavior is that the mechanical work performed by the cell is optimized for a specific range of substrate stiffness. To illustrate this, we computed the average work W done by the cell as:

$$W = 4F\delta \tag{63}$$

where F and δ are the average force and displacement of focal adhesion, respectively. The number 4 arises due to the fact that the square cell has four focal adhesions. Numerically computing W in terms of spring stiffness clearly shows that an optimum stiffness for our system is located around $k = 1$ nN/μm $< k < 10$ nN/μm as show in Fig. 14, a result that qualitatively correlates well with experimental studies on cardiac cell contractions (Adam et al., 2008). This behavior may be explained by the fact that at low substrate stiffness, very little force is generated by cells ($F \to 0$) and thus no work is performed while at high stiffness, cell cannot generate substrate deformation ($\delta \to 0$) which also implies a vanishing work. The intermediate substrate stiffness which optimizes both force and displacement is most of the time preferable for certain cell phenotypes. Understanding such processes is critical for the design optimized artificial gels for tissue engineering (Adam et al., 2008).

5.4. Effect of cell morphology on cell SF structure

Recent experiments on contractile cells (such as cardiomyocyte) have shown that a strong correlation exists between cell shape and structure (Bray et al., 2008; Parker et al., 2008), indicating that cell function, and in particular contractility, is strongly affected by geometrical factors. This section consists of assessing the prediction of the proposed model in that respect. For this, as a mean of comparison with experimental tests (Bray et al., 2008; Parker et al., 2008; Geisse et al., 2009; Bray et al., 2010), we consider three different cells (Fig. 15) each characterized by their own morphology (square, rectangular and triangular shapes) and focal adhesions distribution. In particular, we assume here that a cell adheres to a rigid substrate at specific locations (cell corners), which results in constraining the motion of material points on adhesion islands, represented by black dots in Fig. 15(a). Initial and boundary conditions are similar to those applied in the previous example.

As depicted in Fig. 15 the proposed model is able to capture the general SF organization observed in experiments for various cell morphology (Bray et al., 2008; Parker et al., 2008; Geisse et al., 2009; Bray et al., 2010). Both Fig. 15(b) and (c) show that SFs are mostly generated in directions that are restricted in terms of elongation, i.e. lines between the adhesion islands. As discussed in the previous section, this is explained by the fact that the rate of cytoskeleton's contraction along these directions is very small (close to zero) and thus promotes contractility and SF generation. Overall, these results indicate that interactions between SF formation and mechanics, as described by the proposed model, are sufficient to accurately reproduce key features of cell organization and force generation observed in the experiments.

6. Concluding remarks

To summarize, this paper presents a mixture framework that aims at describing the processes by which contractile cells are able to sense their mechanical environment (through stiffness) and react by adjusting the amount of contractile force they generate. By describing the cell's body as a mixture of four critical contractile elements, the proposed model is able to accurately capture the interplay between both mechanical and chemical mechanisms taking place in cells. The key features of the approach are:

- SF contraction is described by the velocity–tension and length–tension relationships arising from cross-bridge dynamics.
- SF formation arises from mass exchange with dispersed globular actin monomers and is assumed to depend on the tension in existing SF. This aspect is the main assumption of the model regarding the mechano-sensitivity of contraction. Cytosol and globular actin transport is described by conventional diffusion–convection type laws.
- Cell contraction is described in terms of both passive elasticity of the cytoskeleton and active contractile stress from a statistical distribution of SF.

Bischofs, I.B., Klein, F., Lehnert, D., Bastmeyer, M., Schwarz, U.S., 2008. Filamentous network mechanics and active contractility

Tsuda, Y., Yasutake, H., Ishijima, A., Yanagida, T., 1996. Torsional rigidity of single actin laments and actin–actin bond breaking force under torsion measured directly by in vitro micromanipulation. PNAS 93, 12937–12942.

Vernerey, F.J., 2010. On the application of multiphasic theories to the problem of cell-substrate mechanical interactions. Advances in Cell Mechanics.

Vernerey, F.J., Farsad, M., 2011. An Eulerian/xfem formulation for the large deformation of cortical cell membrane. Computer Methods in Biomechanics and Biomedical Engineering 14 (5), 433–445.

Vernerey, F.J., Greenwald, E., Bryant, S., 2011. Triphasic mixture model of cell-mediated enzymatic degradation of hydrogels. Computer Methods in Biomechanics and Biomedical Engineering (in press).

Vernerey, F.J., Liu, W.K., Moran, B., 2007. Multi-scale micromorphic theory for hierarchical materials. Journal of the Mechanics and Physics of Solids 55, 2603–2651.

Wang, H.B., Dembo, M., Wang, Y.L., 2000. Substrate exibility regulates growth and apoptosis of normal but not transformed cells. American Journal of Physiology—Cell Physiology 279, C1345–C1350.